East European Journal of Physics. **1.** 476-484 (2024)
DOI:10.26565/2312-4334-2024-1-52 ISSN 2312-4334

SPECTRA OF ULTRASOUND DOPPLER RESPONSE USING PLANE-WAVE COMPOUNDING TECHNIQUE

Evgen A. Barannik, Mykhailo O. Hrytsenko*
Department of Medical Physics and Biomedical Nanotechnologies, V.N. Karazin Kharkiv National University
4 Svobody Sq., 61022, Kharkiv, Ukraine
**Corresponding Author e-mail: mykhailo.hrytsenko@student.karazin.ua*
Received January 3, 2024; revised February 8, 2024; accepted February 19, 2024

Within the framework of a simple model of the sensitivity function, the Doppler spectra are considered for different ways of generating response signals using plane wave compounding. A Doppler spectrum is obtained for coherent compounding of signals received at different steering angles of waves during their period of changing. Compared to traditional diagnostic systems, the Doppler spectrum width is increased only by limiting the duration of the signals. There is no additional increase in the spectrum width if the compound signals are formed by adding with cyclic permutation, in which signals from each new wave angle are compounded. When a Doppler signal is formed directly from Doppler signals at different steering angles, the spectral width increases both in comparison with the traditional method of sensing with stationary focused ultrasound fields and with the case of coherent signal compouding. The obtained increase in the spectral width has an intrinsic physical meaning. The increase in width is connected with a dynamic change in the Doppler angle, which increases the interval of apparent projections of the velocities of motion of inhomogeneities along the direction of transmitting of a plane wave without inclination.
Keywords: *Ultrasound; Doppler spectrum; Plane wave compounding; Synthetic aperture method; Spectral dispersion; Projection of the inhomogeneity velocity*
PACS: 43.28.Py, 43.35.Yb, 43.60.-c, 87.63.D-, 87.63.dk

INTRODUCTION

As it is known in traditional ultrasound medical diagnostic systems, focused waves have a focus on one strictly defined depth in the patient's body [1,2]. This approach has a number of disadvantages connected with resolution limitations outside the defined focal area and the inability to obtain sufficient data to accurately determine the flow of biological fluids and the structure of the body's subcutaneous biological structures, including tendons, muscles, blood vessels and internal organs. The image is acquired sequentially along one line, which imposes a strict limit on the frame rate, which is important in a real-time imaging system. A low frame rate means that fast-moving structures (e.g. heart valves) are difficult to image continuously in time. The general idea behind synthetic aperture in ultrasound diagnostics is that the ultrasound response is recorded by all elements of the ultrasound transducer for a sequence of different emitted wave fields. The response for each point in space is then identified as a complex value for the different fields, which is coherently summed, resulting in a high-resolution image (with focus) at each point in space [3].

The synthetic aperture method requires a lot of calculations, and as a result, such equipment is expensive [4, 5]. There is a demand for methods that can be integrated directly into existing commercial ultrasound devices [6, 7]. Moreover, it is necessary to optimize the parameters that characterize the quality of images obtained using aperture synthesis technology [8-15]. The method has been significantly developed with the advent of ultrasound scanners that use parallel signal processing to generate images. Along with the use of multilinear data processing in ultrasound diagnostics, it became possible to visualize vital blood flows, which, in comparison with conventional Doppler methods, allowed for the development of methods to determine the velocity vector [16-18], simultaneously visualize blood flow and vessel wall motion in arteries, visualize low-velocity blood flow in small vessels, and perform three-dimensional imaging for all Doppler techniques (color Doppler, 3-D ultrafast energy Doppler, pulsed Doppler, etc.) [19-21, 8].The effect of the movement of ultrasonic scatterers on the correlation function of the Doppler signal and the ways to correct the effect of this impact were investigated in [22, 23]. Using the synthetic aperture method, it is possible to implement imaging methods that use plane waves with different propagation directions or wave fronts with different spatial configurations [24-26,9,12]. This made it possible to generate full-field tissue displacement images and Doppler images with high frame rate and high resolution for various medical applications in modern shear-wave elastography, Doppler ultrasound [27,20,11], etc. The development of methods for coherent compounding of ultrasound response signals has improved spectral estimates in spectral Doppler compared to traditional Doppler techniques. This makes it possible to estimate local pulse wave velocities, visualize contrast agents, etc. [28-30]. There are a number of experimental works on new techniques within the plane wave compounding method that allow to improve image quality in terms of lateral resolution and contrast-to-noise ratio for two-dimensional images [31,32] and for Doppler technique [33].

The width of the Doppler spectra plays an important role for the accuracy of all pulse Doppler methods. The reason for the increase in the spectrum width and its distortion can be: high gradients of the velocity of inhomogeneities, in

Cite as: E.A. Barannik, M.O. Hrytsenko, East Eur. J. Phys. 1, 476 (2024), https://doi.org/10.26565/2312-4334-2024-1-52

particular, red blood cells, inside the measuring volume, even in laminar blood flows; turbulence of the blood flow, in which the projection of the velocity can change not only the value but also its sign; fluid movement with acceleration, which increases the range of velocities; the influence of speckle noise. Earlier, the model of the effect of inhomogeneity velocity gradients was considered in [39]. Some models of the effect of blood flow turbulence, diffusion of inhomogeneities and dependence of spectral width on the correlation radius of inhomogeneities were proposed in [34], and the effect of accelerated motion of inhomogeneities was considered in [36]. The aim of this paper is to develop and analyze the Doppler spectra and its width using the synthetic aperture technology, namely, plane wave compounding with different methods of forming Doppler response signals.

THEORETICAL MODEL

Within the framework of the continuum model of the biological medium, the low-frequency Doppler signal $e_d(t)$ under the pulsed mode of ultrasound wave emission [34,35] depends on the motion of the density inhomogeneities $\rho(\vec{r},t)$ and compressibility $\beta(\vec{r},t)$. It also depends on the complex sensitivity function $G_p'(\vec{r},t)$ over the emission-receiving field. For the synthetic aperture technology, this value is time-dependent and is determined by the duration of the sensing pulses, the complex amplitude of the transmitted field $G_t'(\vec{r},t)$, with its deviation from a plane wave without inclination and by the complex receiver sensitivity function $G_r'(\vec{r})$:

$$G_p'(\vec{r}) = G_t(\vec{r},t)G_r(\vec{r})b\left(T_1 - \frac{x'}{c_0} - \frac{x'cos\Phi(t)}{c_0}\right), \tag{1}$$

where x' is the distance along the transducer axis from its emitting surface to the origin of the x,y,z coordinate system with the beginning at the sensing depth l_0, as shown in Fig. 1, $b(t)$ is the envelope of the probing pulse, T_1 is the delay in the strobing time relative to each moment of the pulse emission, which determines the probing depth, c_0 is the propagation velocity of the reflected wave beam front along the x' axis, $c_0/cos\Phi(t)$ is the propagation velocity along the x' axis of the incident plane wave front with the deflection angle $\Phi(t)$ of the wave vector. In the most general case of the synthetic aperture technology, the sensitivity function to scattered waves may also depend on time t.

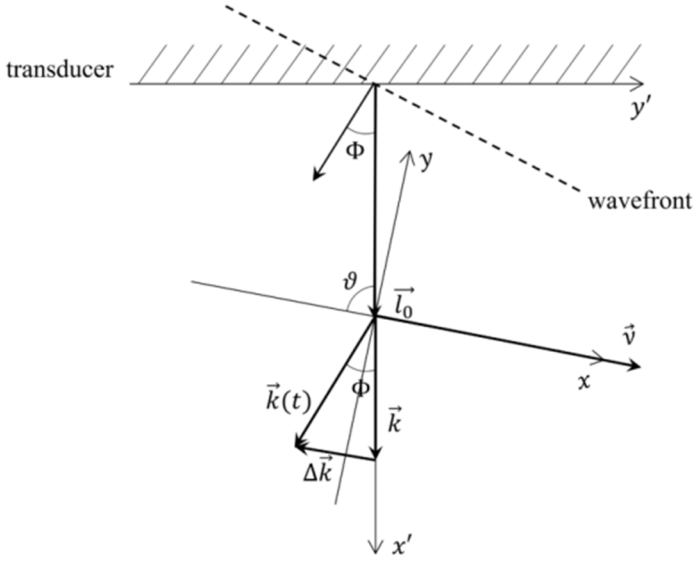

Figure 1. The position of the unshaded coordinate system connected with the measuring volume relative to the ultrasonic transducer and the angle of deflection of the wave vector $\vec{k}(t)$ of the current wave from the wave vector $\vec{k}$ of the wave without inclination

Taking into account the deflection of waves from a plane wave without inclination, the complex amplitude of incident plane waves is given by

$$G_t(\vec{r},t) = e^{i\{\vec{k}(t)-\vec{k}\}\vec{r}}g(z),$$

where $g(z)$ is the distribution of the ultrasonic transmitted field along the z-axis perpendicular to the (x,y) plane shown in Fig. 1. The time dependence is caused by small deviations of the wave vector from the wave vector of plane waves without inclination. Earlier [35], in this approximation, the Fourier image of the function $G_t(\vec{r},t)$ was found with a linear dependence on time of the wave vector deflection angle $\Phi(t) = \Omega t$.

Most conventional pulse systems use sequential emission of pulses characterized by the same spatial geometry and configuration of wavefronts. This means that in this case, the functions $G_t'(\vec{r})$ and $G_r'(\vec{r})$ are time-independent, and the Doppler spectrum has the form [34]:

$$S(\omega_p) = \frac{k^4}{(2\pi)^3}\int d\vec{q}C(\vec{q},\omega_p)\left|G(\vec{q}+2\vec{k})\right|^2 \tag{2}$$

where $C(\vec{q},\omega_p)$ is the space-time Fourier image of the function of the inhomogeneity fluctuation correlator

$$C(\vec{r}_1-\vec{r}_0,\tau)=\nu\left\langle\left(\tilde{\beta}-\tilde{\rho}\right)^2\right\rangle\delta(\vec{r}_1-\vec{r}_0-\tau\vec{V}),$$

ν is a constant determined by the radius of correlation of the inhomogeneities and $\vec{V}$ is the velocity of the dimensionless inhomogeneities $\tilde{\beta}$ and $\tilde{\rho}$.

In the case of the synthetic aperture technology, it is possible to generate an ultrasonic Doppler response signal directly from discrete signal values from different sequential angles of revolution of the wave vector. For a given range of angles Φ, the ultrasonic Doppler response signals are registered for a limited period of time, after which the registration procedure is repeated periodically. Then the power spectrum of the Doppler signal is equal to [36, 37]

$$S(\omega_p)=\frac{k^4}{(2\pi)^3}\sum_{j=-\infty}^{\infty}\int d\vec{q}C(\vec{q},\omega_p-\omega_j)\left|G(\vec{q}+2\vec{k},\omega_j)\right|^2. \quad (3)$$

where $\omega_p=2\pi p/T$ is the Fourier expansion variable, and T is the period of repeating a given set of deflection angles.

There is another way to generate an ultrasonic Doppler signal. Discrete values are obtained by coherent compounding of complex signal values at different angles of rotation for the entire period of angle change T. Then the spectrum can be written as follows [37]:

$$S(\omega_p)=T^2\frac{k^4}{(2\pi)^3}\int d\vec{q}C(\vec{q},\omega_p)\left|G(\vec{q}+2\vec{k},0)\right|^2 \quad (4)$$

$$G(\vec{q}+2\vec{k},0)=\frac{1}{T}\int_{-\frac{T}{2}}^{\frac{T}{2}}G(\vec{q}+2\vec{k},t+t')dt'.$$

Within the framework of the model described in [35-37], it follows from (4) that in this case the sensitivity function is independent of frequency similar to (2).

RESULTS

To reduce the effect of the rectangular window spectrum (which for periodic functions is formed by limiting the integration to $\pm T/2$ limits) on the calculated spectra weight windows are used. In particular, the Gaussian weighting window, which has the following form.

$$W(\tau)=\exp(-\tau^2/T_W^2), \quad (5)$$

where $2T_W\cong T$ is the length of the window along the e^{-1} level. Taking into account the weighting window (5), the integrals over time τ converge well at $\tau\to\pm\infty$. This makes it possible to extend the integration limits to $\pm\infty$ when calculating the spectra. In this approximation, the spectrum of the correlation function of inhomogeneity fluctuations takes the form:

$$C(\vec{q},\omega_p)=\nu\left\langle\left(\tilde{\beta}-\tilde{\rho}\right)^2\right\rangle\sqrt{\pi T_W^2}e^{-\frac{T_W^2(\vec{q}\vec{V}-\omega_p)^2}{4}}. \quad (6)$$

Using (5), it is possible to obtain a sensitivity function with completely suppressed side lobes, unlike in [35]:

$$G_t(\vec{r},\omega_j)=T^{-1}g(z)\sqrt{\pi T_W^2}e^{-\frac{T_W^2(k\Omega y'+\omega_j)^2}{4}}. \quad (7)$$

The resulting expressions (6) and (7) allow us to write the spectrum (3) in the form:

$$S(\omega_p)=\nu\left\langle\left(\tilde{\beta}-\tilde{\rho}\right)^2\right\rangle T^{-1}\sqrt{\pi T_W^2}\frac{k^4}{(2\pi)^3}\sum_{j=-\infty}^{\infty}\int d\vec{q}e^{-\frac{T_W^2(q_xV-\omega_p+\omega_j)^2}{4}}\left|G(q_x+2kcos\vartheta,q_y-2ksin\vartheta,q_z,\omega_j)\right|^2. \quad (8)$$

In expression (8), only the sensitivity function depends on the variables q_y and q_z. Therefore, the inverse Fourier transform can be used to change the function variables to the y,z and simplify the expression. The expression for the contribution of the individual flow lines of the medium to the spectrum can then be written as

$$S(\omega_p,y,z)=\nu\left\langle\left(\tilde{\beta}-\tilde{\rho}\right)^2\right\rangle k^4T^{-1}\sqrt{\pi T_W^2}\sum_{j=-\infty}^{\infty}\int\frac{dq_x}{2\pi}\left|G(q_x+2kcos\vartheta,y,z,\omega_j)\right|^2e^{-\frac{T_W^2(q_xV-\omega_p+\omega_j)^2}{4}}. \quad (9)$$

The flow lines differ in the y and z coordinates and in sum give the full Doppler spectrum. This makes it possible to separate the integration over coordinates from the integration over the wave vector component and summation over frequency.

For further comparison of the spectra, we first obtain an estimate of the spectral distribution for the traditional method of pulsed Doppler sensing. To do this, we will choose the sensitivity function (1) in its simplest form:

$$G(\vec{r}) = exp\left\{-2\frac{y'^2+z^2+(x'-l_0)^2}{a^2}\right\} = exp\left\{-2\frac{\vec{r}^2}{a^2}\right\}. \quad (10)$$

In Equation (10), it is assumed that the waves are plane. That is, we neglect the curvature of the wave fronts, which always occurs due to the focusing and diffraction of ultrasonic waves. In addition, the duration of the probing pulses is chosen such that the measured volume acquires a spherical shape. This approximation is often used to estimate the ultrasonic Doppler response spectra [38,34].

Analogously to (9), using (10), we obtain the spectrum of the Doppler response signal of the flow line in the form

$$S(\omega_p, y, z) = \nu\left\langle\left(\tilde{\beta}-\tilde{\rho}\right)^2\right\rangle T^{-1}k^4\sqrt{\pi T_W^2}\frac{\pi a^2}{2}exp\left\{-4\frac{y^2+z^2}{a^2}\right\}\times$$

$$\times\int\frac{dq_x}{2\pi}exp\left\{-\frac{(q_x+2kcos\vartheta)^2a^2}{4}-\frac{T_W^2\left(q_xV-\omega_p\right)^2}{4}\right\}$$

Then the full spectrum of the Doppler signal is obtained after integration over the coordinates of the flow lines:

$$S(\omega_p) = \nu\left\langle\left(\tilde{\beta}-\tilde{\rho}\right)^2\right\rangle T^{-1}k^4\sqrt{\pi T_W^2}\frac{\pi^2a^4}{8}\int\frac{dq_x}{2\pi}exp\left\{-\frac{(q_x+2kcos\vartheta)^2a^2}{4}-\frac{T_W^2(q_xV-\omega_p)^2}{4}\right\}.$$

Finally, after integration over q_x, we obtain the final formula for the Doppler spectrum:

$$S(\omega_p) = \nu\left\langle\left(\tilde{\beta}-\tilde{\rho}\right)^2\right\rangle T^{-1}k^4\frac{\pi^3a^3}{4}\sqrt{\frac{T_W^2a^2}{a^2+T_W^2V^2}}exp\left\{-\frac{T_W^2a^2}{a^2+T_W^2V^2}\frac{(\omega_p-\omega_d)^2}{4}\right\}, \quad (11)$$

$$\sigma^2 = 2\frac{a^2+T_W^2V^2}{T_W^2a^2} = 2\left(\frac{1}{T_W^2}+\frac{V^2}{a^2}\right), \quad (12)$$

where $\omega_d = -2kVcos\vartheta$ is the Doppler shift frequency, σ^2 is the dispersion of the Doppler frequency spectrum.

In the case of coherent accumulation of signals obtained at different sensing angles, it follows from expressions (4) and (7) that the Doppler spectrum is determined by the amplitude of the incident plane waves. So, it can be written in the following form.

$$G_t(\vec{r}, \omega_j = 0) = T^{-1}\sqrt{\pi T_W^2}e^{-\frac{1}{4}T_W^2k^2\Omega^2y'^2-\frac{z^2}{a^2}}.$$

In physical terms, synthetic aperture technologies are designed to improve resolution. Therefore, it is expediently to choose a value of the maximum angle $T_W\Omega$ of the wave vector deviation at which $\frac{1}{4}T_W^2\Omega^2k^2 = \frac{1}{4}\Phi_{max}^2k^2 = a^{-2}$. In this case, the resolution is not worse than resolution of traditional Doppler systems. In addition, it is possible to get transmit focusing at all points of the biological object at all depths. As a result, the full model sensitivity function can be represented in a form similar to (10)

$$G(\vec{r}, \omega_j = 0) = G_t(\vec{r}, \omega_j = 0)G_r(\vec{r})b\left(T_1-\frac{2x'}{c_0}\right) = T^{-1}\sqrt{\pi T_W^2}\exp\left(-2\frac{\vec{r}^2}{a^2}\right),$$

and the expression for the Doppler spectrum is obtained in a similar way to (11) and has the form

$$S(\omega_p) = \nu\left\langle\left(\tilde{\beta}-\tilde{\rho}\right)^2\right\rangle T^{-1}T_W^2k^4\frac{\pi^4a^3}{4}\sqrt{\frac{T_W^2a^2}{a^2+T_W^2V^2}}exp\left\{-\frac{(\omega_p-\omega_d)^2}{2\sigma^2}\right\}. \quad (13)$$

This spectrum differs only in the higher amplitude of the spectrum due to the increased power of the Doppler response due to the coherent accumulation of signals.

For the ultrasonic Doppler response, when the signal is formed directly from the Doppler signals received at different steering angles, the full sensitivity function can be written as:

$$G(x, y, z, \omega_j) = T^{-1}\sqrt{\pi T_W^2}e^{-\frac{T_W^2\left(k\Omega y'+\omega_j\right)^2}{4}}e^{-\frac{x^2+y^2+2z^2+(x'-l_0)^2}{a^2}}.$$

As with the finding of the spectrum (13), we assume that the equality $\frac{1}{4}\Phi_{max}^2k^2 = a^{-2}$ holds. As a result, we obtain

$$\left|G\left(q_x+2kcos\vartheta,y,z,\omega_j\right)\right|=T^{-1}\sqrt{\pi T_W^2}exp\sqrt{\frac{\pi a^2}{2}}\left(-\frac{1}{4}T_W^2\omega_j^2\right)\times$$

$$\times exp\left\{-\frac{2y^2+T_W\omega_j acos\vartheta y+2z^2}{a^2}\right\}\times exp\left\{-\frac{(q_x+2kcos\vartheta)^2a^2-(T_W\omega_j sin\vartheta)^2}{8}\right\}.$$

Using expression (9), we can now find the full spectrum and write it in the form. Let's take out of the integral over the coordinate all the factors that do not depend on y, z:

$$S\left(\omega_p\right)=\nu\left\langle\left(\tilde{\beta}-\tilde{\rho}\right)^2\right\rangle k^4T^{-3}\pi T_W^2\sqrt{\pi T_W^2}\frac{\pi a^2}{2}\sum_{j=-\infty}^{\infty}exp\left\{\frac{sin\vartheta^2T_W^2\omega_j^2}{4}\right\}\times$$

$$\times exp\left\{-\frac{T_W^2\omega_j^2}{2}\right\}\iint dydz\,exp\left\{-2\frac{2y^2+T_W\omega_j acos\vartheta y+2z^2}{a^2}\right\}\times$$

$$\times\int\frac{dq_x}{2\pi}exp\left\{-\frac{T_W^2\left(q_xV-\omega_p+\omega_j\right)^2}{4}\right\}exp\left\{-\frac{(q_x+2kcos\vartheta)^2a^2}{4}\right\}.$$

Finally, after integration over y and z, we obtain the full Doppler spectrum for the case under consideration, which can be presented in a form similar to (11) and (13):

$$S\left(\omega_p\right)=\nu\left\langle\left(\tilde{\beta}-\tilde{\rho}\right)^2\right\rangle k^4T^{-3}T_W^2\frac{\pi^3a^3}{8}\sqrt{\frac{T_W^2a^2}{a^2+T_W^2V^2}}\sum_{j=-\infty}^{\infty}exp\left\{-\frac{1}{4}T_W^2\omega_j^2\right\}exp\left\{-\frac{T_W^2a^2}{a^2+T_W^2V^2}\frac{\left(\omega_p-\omega_d-\omega_j\right)^2}{4}\right\}$$

It is easy to see that for the component of the sum with $j=0$ and, accordingly, with $\omega_j=0$, this expression transforms to the spectrum of (11) and (13) with an accuracy of a numerical factor.

An estimate of the full spectrum of the Doppler response signal can now be obtained by summing over j. If the measurement period T is sufficiently long, then the frequency step $2\pi/T$ in the Fourier transform is small. This means that the sum over j can be replaced by a frequency integral according to the rule

$$\sum_{j=-\infty}^{\infty}\ldots\rightarrow\frac{T}{2\pi}\int_{-\infty}^{\infty}\ldots d\omega,$$

As a result, after some simple but cumbersome calculations, we come to the final expression for the ultrasonic Doppler response spectrum:

$$S\left(\omega_p\right)=\left\langle\left(\tilde{\beta}-\tilde{\rho}\right)^2\right\rangle k^4T^{-2}T_W^2\frac{\pi^2a^4}{8}\sqrt{\frac{\pi}{2a^2+T_W^2V^2}}exp\left\{-\frac{T_W^2a^2\left(\omega_p-\omega_d\right)^2}{4\left(2a^2+T_W^2V^2\right)}\right\}. \tag{14}$$

The dispersion of this Doppler spectrum

$$\sigma^2=2\frac{2a^2+T_W^2V^2}{T_W^2a^2}=2\left(\frac{2}{T_W^2}+\frac{V^2}{a^2}\right),$$

is greater than the dispersion (12) of the spectra (11) and (13) by $\Delta\sigma^2=2/T_W^2$.

DISCUSSION

The considered simple physical model for the sensitivity function demonstrates that, in general, the contribution to the spectral width of the Doppler signal is made not only by the parameters of the incident and reflected ultrasonic fields, which form the sensitivity function, but also by the signal duration. The spectral characteristics of the inhomogeneity fluctuation correlator depend on the signal duration. If the width of the weighting window is large, then in the limiting case $T_W\rightarrow\infty$, the spatial spectrum of the fluctuation correlator (6) is described by the δ-function

$$C(\vec{q},\omega)=2\pi\nu\left\langle\left(\tilde{\beta}-\tilde{\rho}\right)^2\right\rangle\delta\left(\vec{q}\vec{V}-\omega_p\right),$$

which, when integrated over q_x, equates its value to $q_x=\omega_p/V$. In this case, the largest contribution to the width of the spectra (11), (13), and (14) will be made by the component $2V^2/a^2$, which is related to the value $\sqrt{2}a$, which, according to (10), determines the diameter of the measuring volume at the level of e^{-1}.

On the contrary, as the measuring volume increases ($a \to \infty$), the dispersion of the spectra (11) and (13) tends to $2/T_W^2$, and dispersion of the spectrum (14) to $4/T_W^2$, i.e., it is determined by the duration of the weighting window, which effectively limits the length of the Doppler signal. In this case, the spectrum of the sensitivity function becomes δ-shaped, which equals $q_x = -2k cos\vartheta$. However, in both cases, the maximum of the Doppler spectra (11), (13) and (14) is always at the classical Doppler shift frequency ω_d. In traditional pulsed ultrasound diagnostic systems, sequential pulses with a constantspatial geometry and configuration of wavefronts are used. In this case, Doppler signals are practically unlimited in time and therefore the spectral width is the smallest possible and does not depend on T_w.

The reason for the increase in the width of the Doppler spectrum when forming a signal from Doppler signal counts obtained at different steering angles is the change in the projection of the motion velocity onto the direction of the current wave vector due to a change in the Doppler angle, as shown in Fig. 2. This situation can be interpreted as a movement with acceleration:

$$V_{x'} = Vcos\vartheta(t) = Vcos(\vartheta \mp \Phi) = V(cos\vartheta cos\Phi \pm sin\vartheta sin\Phi) \cong V\{cos\vartheta \pm sin\vartheta\Omega t\},$$

where the upper sign describes a situation equivalent to a uniformly accelerated motion, and the lower sign corresponds to a uniformly decelerated motion.

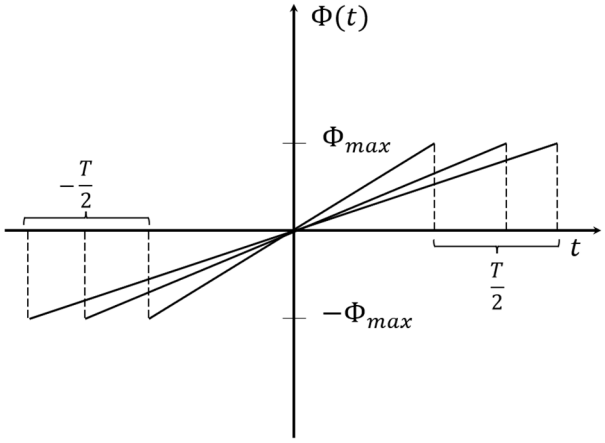

Figure 2. Model dependence of the wave vector deflection angle on time

In practice, the width of the weight window satisfies the ratio $T_w \cong T/2$. And the rate of change of the angle of view can be represented as $\Omega = 2\Phi_{max}/T$. Then the projection of the velocity on the x' axis is equal:

$$V_{x'} = Vcos\vartheta \pm Vsin\vartheta \frac{\Phi_{max}}{T_w} t\,.$$

Thus, the notional acceleration is inversely proportional to the time T_w. It is clear that both during acceleration and deceleration, the range of velocities during time T for a given range of angles is the same, so the width of the spectrum cannot depend on the sign of the acceleration. Because of this, in (14), compared to (13), there is a quadratic acceleration term in the form of $2/T_W^2$. From Fig. 2, it is easy to see that the larger T and, accordingly, T_w, the smaller the acceleration at a given range of angles Φ_{max}, the smaller the range of velocities and, accordingly, the additional dispersion of the Doppler frequency spectrum. Obviously, such terms can be neglected when the strong inequality $1/T_W^2 \ll V^2/a^2$ is satisfied.

Fig. 3 schematically shows the dependence of the complex ultrasonic Doppler response signal on time when the inclination of $N = 3$ transmitted plane waves is periodically repeated. If the velocity $V_{x'}$ apparently increases due to a decrease in the angle $\vartheta(t)$, then for each subsequent time interval $\Delta T = T/N = t_n - t_{n-1}$ between probings, the phase difference of the complex Doppler signals will also increase: $\Delta\varphi_n = 2k\Delta x'_n = 2kV_{x'}\Delta T$. It is this apparent increase in the range of differential phases $\Delta\varphi_n$ that leads to an increase in the spectral width (14). In accordance with (4) a compound signal can be written as follows:

$$e_c(t_n) = \sum_{m=-(N-1)/2}^{(N-1)/2} e_d(t_{n+m}), \tag{15}$$

and Fig. 3 shows that the phase difference for two consecutive compound signals e_c remains unchanged. This means that, unlike (14), there is no additional increase in the spectral width if the compound signals e_c are formed by cyclic permutation taking into account the signal at every new angle. This important circumstance means that accurate measurements of the velocity are possible not only using the compound signals of the form

$$e_c(\mathbf{n^i}) = e_d(\mathbf{n^i} - (\mathbf{N-1})/\mathbf{2}) + e_d(\mathbf{n^i} - (\mathbf{N-3})/\mathbf{2}) + \ldots + e_d(\mathbf{n^i}) + \ldots + e_d(\mathbf{n^i} + (\mathbf{N-3})/\mathbf{2}) + e_d(\mathbf{n^i} + (\mathbf{N-1})/\mathbf{2}),$$

but also, those obtained by cyclic permutation (15). This means that no time is lost in obtaining the entire set of response signals for waves with different inclinations.

Note that the results presented here are based on a linear approximation of the time dependence of the deviation of the wave vector $\Delta\vec{k}(t) = \vec{k}(t) - \vec{k}$. This means that only the projection of the vector $\Delta\vec{k}(t)$ onto the y'-axis was taken into account [35], which is small due to the small values of the angles $\Phi(t)$. At the same time, this vector also has a projection on the x' axis, which depends on the square of time.

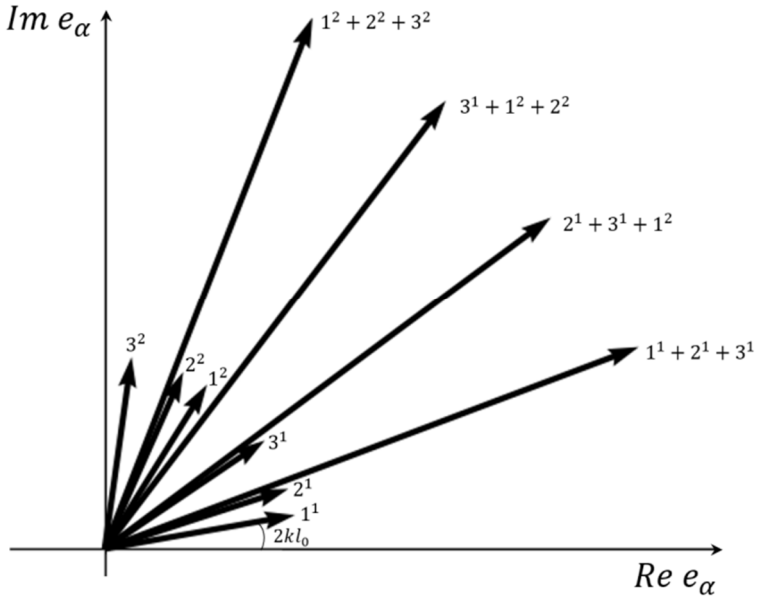

Figure 3. Non-linear time growth of the phase difference $\Delta\varphi_n$ for the complex Doppler signal and the phase difference for the compound signals when the number of different inclination angles is $N = 3$: $\mathbf{n^i}$ **-** Doppler response signal e_d at the **n**-th inclination angle at the **i**-th probing period; $\mathbf{1^1+2^1+3^1}$, $\mathbf{2^1+3^1+1^2}$, $\mathbf{3^1+1^2+2^2}$, $\mathbf{1^2+2^2+3^2}$… **-** compound signals e_c obtained by cyclic permutation taking into account the signal from each new angle, as described by expression (15).

The importance of taking into account such quadratic terms is due to the fact that not only the spectrum of the ultrasonic Doppler response signal, but also the resolution of the system formed by the plane wave compounding technology may depend on them.

CONCLUSIONS

The technology of plane wave compounding uses a periodic repetition of the sequence of waves with different inclinations. Therefore, a periodic extension of all time-dependent physical parameters naturally occurs, which leads to a limitation of the duration of ultrasonic Doppler response signals. The influence of limiting the duration of the response signals and its anodization by weight windows on the spectral properties of the correlator of inhomogeneity motion and the spectrum of the sensitivity function of the ultrasonic system is determined. In contrast to the spectrum of the correlation function, the width of the sensitivity function spectrum depends on both the size of the measuring volume and the duration of the signals.

Within the framework of a simple model of the sensitivity function, the Doppler spectra are considered for different ways of forming response signals using plane wave compounding. A Doppler spectrum is obtained by coherent compounding of signals received at different angles of inclination of waves during their repetition period. Compared to traditional diagnostic systems, the Doppler spectrum width is increased only by limiting the duration of the signals. There is no additional increase in the spectrum width if the compound signals are formed by accumulation with cyclic permutation, in which signals from each new wave angle are added.

When forming a Doppler signal directly from Doppler signals at different inclination angles, the spectral width increases both in comparison with the traditional method of sensing with stationary focused ultrasonic fields and with the case of coherent signal accumulation. In terms of the internal physical meaning, the invented increase in the spectral width is connected with a dynamic change in the Doppler angle, which increases the interval of apparent projections of the velocities of motion of inhomogeneities along the direction of transmitting of a plane wave without inclination. The influence of nonlinear terms depending on the time of deviation of the wave vector from the wave vector without inclination requires additional study.

The study was supported by the Ministry of Education and Science of Ukraine (grant #0122U001269).

ORCID

Evgen A. Barannik, https://orcid.org/0000-0002-3962-9960; **Mykhailo O. Hrytsenko,** https://orcid.org/0009-0002-5670-5686

REFERENCES

[1] A. Carovac, F. Smajlovic, and D. Junuzovic, Acta Informatica Medica, **19**(3), 168 (2011). https://www.ncbi.nlm.nih.gov/pmc/articles/PMC3564184/
[2] V. Chan, and A. Perlas, "Basics of Ultrasound Imaging," in: *Atlas of Ultrasound-Guided Procedures in Interventional Pain Management*, (Springer: Berlin/Heidelberg, Germany, 2011). pp. 13-19. http://dx.doi.org/10.1007/978-1-4419-1681-5_2
[3] I. Trots, A. Nowicki, M. Lewandowski, and Y. Tasinkevych, *Synthetic Aperture Method in Ultrasound Imaging,* (IntechOpen, London, UK, 2011). http://dx.doi.org/10.5772/15986
[4] S.I. Nikolov, B.G. Tomov, and J.A. Jensen, in: *2006 Fortieth Asilomar Conference on Signals, Systems and Computers*, (Pacific Grove, CA, USA, 2006), pp. 1548-1552. https://doi.org/10.1109/ACSSC.2006.355018
[5] M. Tanter, and M. Fink, IEEE Trans. Ultrason. Ferroelectr. Freq. Control. **61**(1), 102 (2014). https://doi.org/10.1109/TUFFC.2014.6689779
[6] M.A. Lediju, G.E. Trahey, B.C. Byram and J.J. Dahl, IEEE Trans. Ultrason. Ferroelec. Freq. Contr. **58**(7), 1377 (2011). https://doi.org/10.1109/TUFFC.2011.1957
[7] Y.L. Li, and J.J. Dahl, J. Acoust. Soc. Am. **141**(3), 1582 (2017). https://doi.org/10.1121/1.4976960
[8] J. Provost, C. Papadacci, C. Demene, J. Gennisson, M. Tanter, and M. Pernot, IEEE Trans. Ultrason. Ferroelec. Freq. Contr. **62**(8), 1467 (2015). https://doi.org/10.1109/TUFFC.2015.007032
[9] G. Montaldo, M. Tanter, J. Bercoff, N. Benech, and M. Fink, IEEE Trans. Ultrason. Ferroelectr. Freq. Contr. **56**(3), 489 (2009). https://doi.org/10.1109/TUFFC.2009.1067
[10] J. Jensen, M.B. Stuart, and J.A. Jensen, IEEE Trans. Ultrason. Ferroelec. Freq. Contr. **63**(11), 1922 (2016). https://doi.org/10.1109/TUFFC.2016.2591980
[11] C. Papadacci, M. Pernot, M. Couade, M. Fink, and M. Tanter, IEEE Trans. Ultrason. Ferroelec. Freq. Contr. **61**(2), 288 (2014). http://doi.org/10.1109/TUFFC.2014.6722614
[12] J. Cheng, and J.Y. Lu, IEEE Trans. Ultrason. Ferroelec. Freq. Contr. **53**(5), 880 (2006). https://doi.org/10.1109/TUFFC.2006.1632680
[13] N. Oddershede, and J.A. Jensen, IEEE Trans. Ultrason. Ferroelec. Freq. Contr. **54**(9), 1811 (2007). https://doi.org/10.1109/TUFFC.2007.465
[14] B. Denarie et al., IEEE Trans. Med. Imaging, **32**(7), 1265 (2013). https://doi.org/10.1109/TMI.2013.2255310
[15] R. Moshavegh, J. Jensen, C.A. Villagómez-Hoyos, M.B. Stuart, M.C. Hemmsen, and J.A. Jensen, in: *Proceedings of SPIE Medical Imaging*, (San Diego, California, United States, 2016) pp. 97900Z-97900Z-9. https://doi.org/10.1117/12.2216506
[16] J.A. Jensen, and N. Oddershede, IEEE Trans. Med. Imag. **25**(12), 1637(2006). https://doi.org/10.1109/TMI.2006.883087
[17] J. Udesen, F. Gran, K.L. Hansen, J.A. Jensen, C. Thomsen, and M.B. Nielsen, IEEE Trans. Ultrason. Ferroelec. Freq. Contr. **55**(8), 1729 (2008). https://doi.org/10.1109/TUFFC.2008.858
[18] S. Ricci, L. Bassi and P. Tortoli, IEEE Trans. Ultrason. Ferroelec. Freq. Contr. **61**(2), 314 (2014).https://doi.org/10.1109/TUFFC.2014.6722616
[19] Y.L. Li, and J.J. Dahl, IEEE Trans. Ultrason. Ferroelec. Freq. Contr. **62**(6), 1022 (2015). https://doi.org/10.1109/TUFFC.2014.006793
[20] J. Bercoff, G. Montaldo, T. Loupas, D. Savery, F. Meziere, M. Fink, and M. Tanter, IEEE Trans. Ultrason. Ferroelec. Freq. Contr. **58**(1), 134 (2011).https://doi.org/10.1109/TUFFC.2011.1780
[21] Y.L. Li, D. Hyun, L. Abou-Elkacem, J. K. Willmann, J.J. Dahl, IEEE Trans. Ultrason. Ferroelec. Freq. Contr. **63**(11), 1878 (2016). https://doi.org/10.1109/TUFFC.2016.2616112
[22] D. Hyun, and J.J. Dahl, J. Acoust. Soc. Am. **147**(3), 1323 (2020). https://doi.org/10.1121/10.0000809
[23] I.K. Ekroll, M.M. Voormolen, O.K.-V. Standal, J.M. Rau, and L. Lovstakken, IEEE Trans. Ultrason. Ferroelec. Freq. Contr. **62**(9), 1634 (2015). https://doi.org/10.1109/TUFFC.2015.007010
[24] J.A. Jensen, S.I. Nikolov, K.L. Gammelmark, and M.H. Pedersen, Ultrasonics, **44**(1), e5 (2006). https://doi.org/10.1016/j.ultras.2006.07.017
[25] M. Tanter, J. Bercoff, L. Sandrin, and M. Fink, IEEE Trans. Ultrason. Ferroelectr.Freq. Contr. **49**(10), 1363 (2002). https://doi.org/10.1109/TUFFC.2002.1041078
[26] J.-l. Gennisson, et al., IEEE Trans. Ultrason. Ferroelec. Freq. Contr. **62**(6), 1059 (2015). https://doi.org/10.1109/TUFFC.2014.006936
[27] J. Bercoff, M. Tanter, and M. Fink, IEEE Trans. Ultrason. Ferroelec. Freq. Contr. **51**(4), 396 (2004). https://doi.org/10.1109/TUFFC.2004.1295425
[28] H. Hasegawa, and H. Kanai, IEEE Trans. Ultrason. Ferroelec. Freq. Contr. **55**(12), 2626 (2008). https://doi.org/10.1109/TUFFC.2008.978
[29] J. Vappou, J. Luo, and E.E. Konofagou, Am. J. Hypertens. **23**(4), 393 (2010). https://doi.org/10.1038/ajh.2009.272
[30] O. Couture, M. Fink, and M. Tanter, IEEE Trans. Ultrason. Ferroelec. Freq. Contr. **59**(12), 2676 (2012). https://doi.org/10.1109/TUFFC.2012.2508
[31] C. Zheng, Q. Zha, L. Zhang, and H. Peng, IEEE Access, **6**, 495 (2018). https://doi.org/10.1109/ACCESS.2017.2768387
[32] Y.M. Benane, et al., in: 2017 *IEEE International Ultrasonics Symposium (IUS)*, (Washington, DC, USA, 2017). pp. 1-4. https://doi.org/10.1109/ULTSYM.2017.8091880
[33] C.-C. Shen, and Y.-C. Chu, Sensors, **21**, 4856 (2021). https://doi.org/10.3390/s21144856
[34] I.V. Skresanova, and E.A. Barannik, Ultrasonics, **52**(5), 676 (2012). https://doi.org/10.1016/j.ultras.2012.01.014
[35] I.V. Sheina, and E.A. Barannik, East Eur. J. Physics, (1), 116 (2022). https://doi.org/10.26565/2312-4334-2022-1-16
[36] E.A. Barannik, and O.S. Matchenko, East Eur. J. Phys. **3**(2) 61 (2016). https://doi.org/10.26565/2312-4334-2016-2-08 (in Russian)
[37] I.V. Sheina, O.B. Kiselov, and E.A. Barannik, East Eur. J. Phys. (4), 5 (2020). https://doi.org/10.26565/2312-4334-2020-4-01
[38] C.A.C. Bastos, P.J. Fish, R. Steel, and F. Vaz, Ultrasonics, **37**(9), 623–632 (2000). https://doi.org/10.1016/S0041-624X(00)00004-4
[39] E.A. Barannik, Acoust. Phys. **43**(4), 387 (1997). http://www.akzh.ru/pdf/1997_4_453-457.pdf. (in Russian)

СПЕКТРИ СИГНАЛІВ УЛЬТРАЗВУКОВОГО ДОППЛЕРІВСЬКОГО ВІДГУКУ ПРИ ВИКОРИСТАННІ ТЕХНОЛОГІЇ КОМПАУНДИНГА ПЛАСКИХ ХВИЛЬ

Євген О. Баранник, Михайло О. Гриценко

Кафедра Медичної Фізики та Біомедичних Нанотехнологій, Харківський Національний університет ім. В.Н. Каразіна, 61022, Україна, м. Харків, м. Свободи, 4

В межах простої моделі функції чутливості розглянуті допплерівські спектри при різних способах формування сигналів відгуку з використанням компаундингу пласких хвиль. Винайдений допплерівський спектр при когерентному компаундингу сигналів, отриманих при різних кутах нахилу хвиль на протязі періоду їх повторення. У порівнянні з традиційними діагностичними системами збільшення ширини допплерівського спектру відбувається тільки за рахунок обмеження тривалості сигналів. Додаткове збільшення ширини спектру відсутнє, якщо компаундні сигнали формуються шляхом накопичення з циклічною перестановкою, при якій додаються сигнали від кожного нового кута нахилу хвиль. При формуванні допплерівського сигналу безпосередньо з допплерівських сигналів при різних кутах нахилу відбувається збільшення ширини спектру як у порівнянні з традиційним методом зондування стаціонарними сфокусованими ультразвуковими полями, так і з випадком когерентного накопичення сигналів. За внутрішнім фізичним змістом винайдене збільшення ширини спектру пов'язане з динамічною зміною допплерівського кута, яке збільшує інтервал позірних проекцій швидкостей руху неоднорідностей вздовж напрямку випромінювання пласкої хвилі без нахилу.

Ключові слова: *ультразвук; допплерівський спектр; метод синтезованої апертури; компаудинг пласких хвиль; дисперсія спектру; швидкість руху неоднорідностей*